ELSEVIER

Chemical Engineering Journal 89 (2002) 173–183

Chemical Engineering Journal

www.elsevier.com/locate/cej

Application of shape factor to determine the permeability of perfusive particles☆

Bader Albusairi, James T. Hsu*

Department of Chemical Engineering, Lehigh University, Bethlehem, PA 18015, USA

Received 25 June 2001; accepted 11 February 2002

Abstract

A modified graphical–statistical method for shape factor estimation has been developed and used to estimate the permeability of a perfusive particle as an example. The shape factor was evaluated by calculating the average cross-sectional area for diffusion and the average flow path line length separately. According to this method, a perfusive particle with a sealing surface length ratio, L_s, of 0.04, i.e. a contact length of the perfusive particle on the walls of the test cell tube to the perfusive particle diameter of 0.04, would have a shape factor of $1.25\pi a$. Then, the graphical–statistical method and the geometrical method were used to propose an expression to evaluate the shape factor of any perfusive particle with a sealing surface length ratio of L_s and a radius of a. Finally, the shape factor approach was compared with the CFD numerical simulation approach of Pfeiffer et al. [AIChE J. 42 (1996) 932], and excellent agreement between the two approaches has been demonstrated.

Keywords: Diffusion; Fluid mechanics; Mass transfer; Particle; Porous media; Shape factor

1. Introduction

Chemical processes adopting perfusive particles as the support for catalyst or adsorbent have been used significantly in the last decade, especially perfusive chromatography. The main feature of the perfusive particles is the macro-interconnected pores, which allow solute to transfer from the mobile phase to the stationary one by convection in addition to the diffusion. Therefore, intraparticle velocity become critical in mass transfer balance and cannot be neglected. This additional transport mechanism has been demonstrated experimentally to enhance the separation of biomolecules such as bovine serum albumin [2,3], β-galactosidase [4] and proteins [5–7].

Intraparticle velocity has been calculated using Darcy's law [2,6,8], using the stream function developed by Neale et al. [9], or by solving Brinkman's equations in both the perfusive particle and its surroundings in the bed [10]. In all of these developed intraparticle velocity expressions, bed permeability, K_b, and perfusive particle permeability, K_P, are the major parameters. The bed permeability, K_b, can be calculated through the traditional correlations. On the other hand, the perfusive particle permeability, K_P, is a new parameter that appears only in perfusive systems. Therefore, a good estimation of perfusive particle permeability, K_P, is an essential issue.

Several investigators have estimated perfusive particle permeability by treating the perfusive particle as a bed of micro-particles. Thus, the Carmen–Kozeny equation, as shown in Eq. (1), can be adopted for estimating the permeability of perfusive particle. In the Carmen–Kozeny equation, K_P is the permeability of perfusive particle, d_m is the equivalent micro-particle diameter, and ε_P is the perfusive particle porosity.

$$K_P = \frac{\varepsilon_P^3 d_m^2}{150(1-\varepsilon_P)^2} \tag{1}$$

The first measurement to the permeability of a single perfusive particle experimentally was reported by Pfeiffer et al. [1]. First, an apparatus capable of measuring the flow in a single perfusive particle at different pressure drops was designed and the results were as shown in Fig. 1. Then, commercial software to predict the flow in a perfusive particle at different values of the permeability was used, as shown in Fig. 2. Finally, by combining the experimental and the

☆ This is a preprint of a paper submitted for publication to Chemical Engineering Journal. Its content should neither be quoted nor referred to without the authors' written permission.

* Corresponding author. Tel.: +1-610-758-4257; fax: +1-610-758-5851.
E-mail address: jth0@lehigh.edu (J.T. Hsu).

1385-8947/02/$ – see front matter
PII: S1385-8947(02)00031-1

Nomenclature

a	radius of perfusive particle
a_s	sealing surface length
A_{avg}, A_{eq}	average and equivalent cross-sectional area, respectively
A'_{kij}	average cross-sectional area of block (ijk)
C	constant
d_m	equivalent diameter of micro-spheres
i	index of flow path line in z-plane
j	index of flow path line in x-plane
k	index of cross-sectional area for flow
K_b	bed permeability value
K_P	particle permeability value
K_{Pi}	particle interstitial (specific) permeability
L	flow path length
L_{avg}, L_{eq}	average and equivalent diffusion path length
L'_{ijk}	average diffusion path length of the block (ijk)
L_s	sealing surface length ratio
m	number of flow path lines in each s x-plane
n	number of cross-sectional area, i.e. number of isobaric lines
p	number of flow path lines in each z-plane
P	pressure
Q	flow rate
Q_{ij}	flow between L_{ij}, $L_{(i+1)j}$, $L_{i(j+1)}$, and $L_{(i+1)(j+1)}$
R_s	shape factor resistance $= 1/S$
S	shape factor
$\bar{S}$	equivalent shape factor
W	weight function
x_0	length of first segment of the flow path length L_1, i.e. L_{111}

Greek letters

ε_P	particle void fraction (particle porosity)
μ	absolute viscosity

simulated results, the permeability of the perfusive particle was predicted.

Using different pressure drops across the perfusive particle than the one specified in Fig. 2 or different nominal diameters of the perfusive particle can be tolerated since Darcy's law is a linear relationship. Meanwhile, the change in particle geometry or other physical conditions such as particle porosity, ε_P, will require to repeat the simulation prediction in [1], thus limiting the benefits of this procedure. In this paper the simulation step will be replaced with a new technique based on the traditional shape factor concept in heat transfer. This technique is simpler in general; especially a single equation can be used to predict the value of the shape factor.

Shape factor is a parameter that has been used to estimate different types of flows in a permeable (conductive) medium. Shape factor can be obtained analytically [11,12], graphically [13,14], geometrically, numerically, experimentally [15], or by any combination of these methods [16].

Heat flow through a furnace wall [17] is the first application, where shape factor concept is used. Since that time, many researchers have spent a lot of time to investigate this concept and its validity for many different shapes [15,18–21]. Heat flow by conduction is the field that benefits most from the shape factor technique, shape factor having originated from the heat conduction problem. In addition, followers have tried to apply the shape factor approach [17], by using the same technique to different medium shapes. And also, heat conduction flow is usually associated more with heat flow in irregular shapes than any other type of flow.

Lacking of use of the shape factor technique in other heat transfer fields does not necessarily mean that this concept cannot be applied to other types of flow. The shape factor technique has been used to estimate the permeability of soils and clays [22,23], to estimate the flow rate of underground water in the infiltration process [24], and to measure the capacitance of several three-dimensional bodies located in an electrical field [25].

Shape factor for any shape depends only on the geometry of that shape and not on the surrounding condition values. Therefore, its value will not change as the potential drop value around it changes. Moreover, it can be used in the regular transport equations by replacing the ratio of the cross-sectional area to the diffusion length with the shape factor.

In this paper, a modified graphical–statistical method for evaluation of shape factor of three-dimensional bodies will be presented. It is modified from the traditional two-dimensional graphical method [13,14]. In addition, it depends on averaging cross-sectional area as well as diffusion path length; therefore, it is called graphical–statistical method. This method was proven to give the value of the shape factor of the shape under study by using electrical network. As an example, this method was applied to the perfusive particle studied in Pfeiffer et al. [1], and it produced excellent agreement with their result. Finally, a general correlation was established for the shape factor for a spherical perfusive particle that was inserted in a tube as in Pfeiffer et al. [1]. This correlation would simplify the determination of the permeability of a single perfusive particle.

2. Theory

Shape factor is used to estimate the steady flow in permeable (conductive) medium between two boundaries. Both boundaries were subjected to constant potentials, but each potential had a different value. Shape factor is mainly the ratio between the average cross-sectional area perpendicular to the flow to the average effective distance for flow travel. It

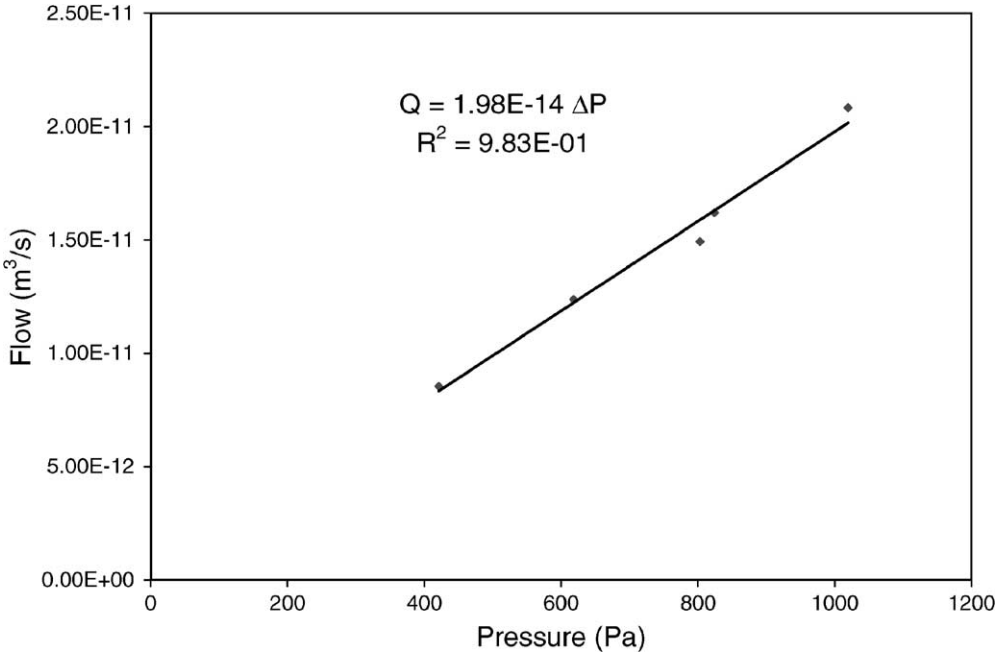

Fig. 1. Data of Pfeiffer et al. [1] represented as flow rate vs. pressure drop.

is used in the flow equation as illustrated in Eq. (2), which is simply Darcy's law with consideration for irregular shapes.

$$Q = \frac{K_P}{\mu} S(-\Delta P), \quad S = \frac{A_{avg}}{L_{avg}} \tag{2}$$

If an experiment can be performed to measure the flow rate, Q, which passes through a perfusive particle at different pressure drop values, as in Pfeiffer et al. [1], then the permeability of the perfusive particle can be obtained through Eq. (3). Therefore, the shape factor, S, for the particle under consideration must be evaluated.

$$K_P = \frac{\mu}{S} \frac{Q}{-\Delta P} \tag{3}$$

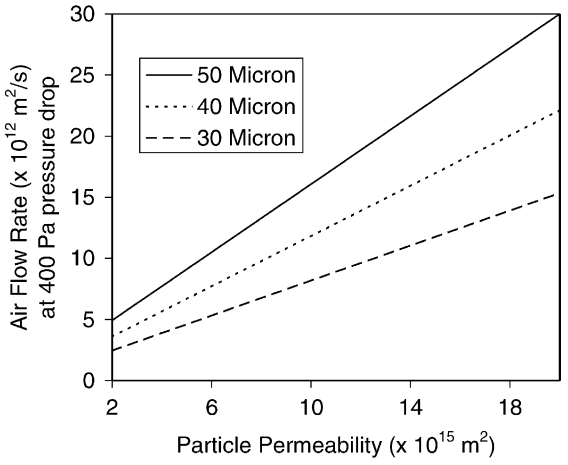

Fig. 2. Volumetric air flow rates as a function of particle permeability for three particle diameters as determined by CFD model at 400 Pa pressure drop (from [1]).

3. Derivation of a modified graphical–statistical shape factor method

Consider any three-dimensional porous body subjected to a pressure drop of ΔP. A flux network of n isobaric lines (n cross-sectional areas) and mp flow path lines can be constructed on it, as represented in Fig. 3A for the j-plane parallel to the flow and Fig. 3B for the k-plane perpendicular to the flow, where L_{ijk} is the segment of flow path line L_{ij} located between cross-sectional areas A_k and A_{k+1} and A_{kij} is the portion of cross-sectional area A_k surrounded by flow path lines L_{ij}, $L_{i(j+1)}$, $L_{(i+1)j}$, and $L_{(i+1)(j+1)}$. The equivalent average cross-sectional area, A_{eq}, and the equivalent average flow path length, L_{eq}, can be estimated by Eqs. (4) and (5), respectively.

$$A_{eq} = \frac{1}{n} \sum_{k=1}^{n} A_k \tag{4}$$

$$L_{eq} = \frac{1}{mp} \sum_{i=1}^{m} \sum_{j=1}^{p} L_{ij} \tag{5}$$

Before beginning this derivation, there are two terms that will be used, the average property and the equivalent average property. For the same body, the latter value is a function of m, p, and n values, while the other one is not. The value of the equivalent average property will converge to the value of the average property as the values of m, p, and n increase; i.e. very condense flux network.

According to the previous two terms, a new definition for the shape factor arises called equivalent shape factor, $\bar{S}$, which is the ratio between the equivalent average

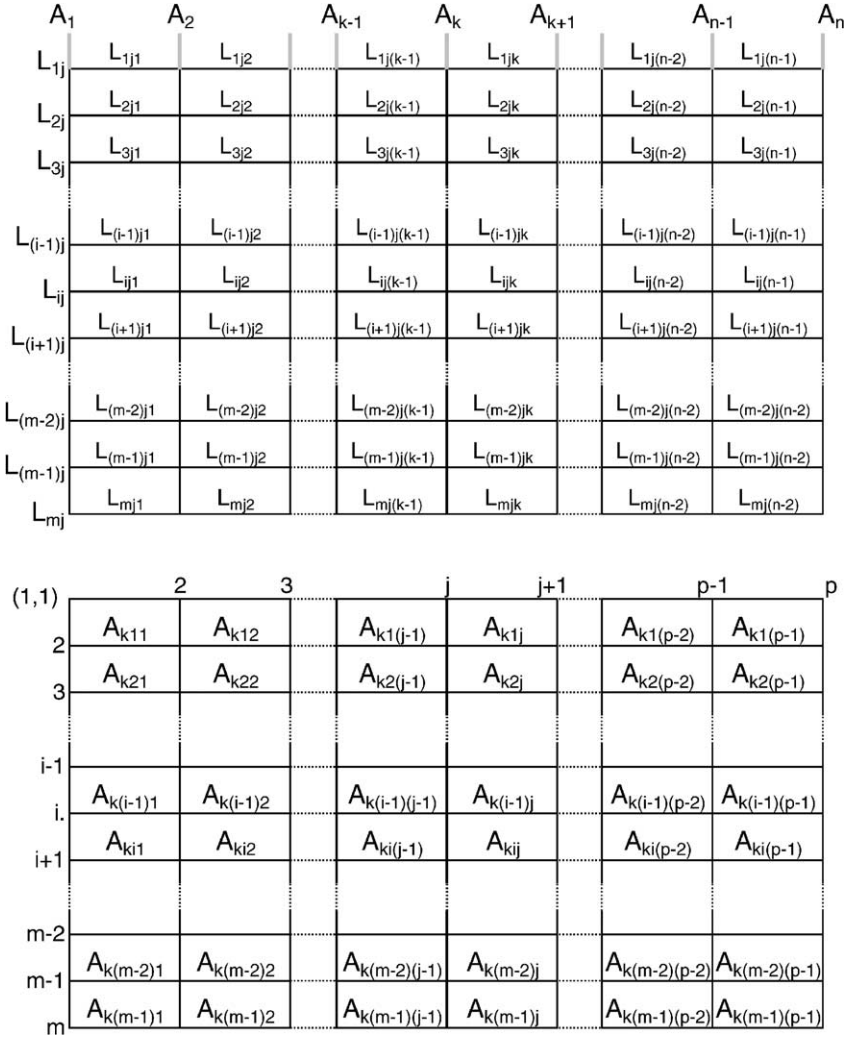

Fig. 3. (A) Plane of the flux network parallel to the flow with constant flow path lines, L_{ij}, and isobaric cross-sectional areas, A_k. (B) Plane of the flux network perpendicular to the flow.

cross-sectional area to the equivalent average flow path length.

3.1. Shape factor

Let R_s be the shape resistance of the medium to the flow, i.e. the reciprocal of the shape factor. If a resistance can represent each block in the flux network, then R_s for the whole shape is the equivalent resistance of all of them. Therefore, by representing R_s as shown in the electrical network in Fig. 4, R_s can be obtained as follows:

$$S = R_s^{-1} = \sum_{i=1}^{m-1}\sum_{j=1}^{p-1}\left[\sum_{k=1}^{n-1} R_{s,ijk}\right]^{-1}, \quad R_{s,ijk} = \frac{L'_{ijk}}{A'_{kij}} \tag{6}$$

where A'_{kij} and L'_{ijk} are the average cross-sectional area and the average flow path length for the block *ijk*, respectively.

Eq. (6) is valid for any shape without any assumptions, the only required information is the ratio L'_{ijk}/A'_{kij} for the entire blocks of the network. In practice, it is not easy to find this ratio for many shapes. Therefore, some reasonable assumptions must be specified to ease the handling of this equation.

First assumption: *select the isobaric lines so that the pressure drop is the same between each of them.* This assumption states that the pressure drop between any two consecutive cross-sectional areas, ΔP_k, is constant for all *k*.

$$S = R_s^{-1} = \sum_{i=1}^{m-1}\sum_{j=1}^{p-1}\left[\sum_{k=1}^{n-1}\frac{1}{C_{ij}}\right]^{-1} = \sum_{i=1}^{m-1}\sum_{j=1}^{p-1}\left[\frac{n-1}{C_{ij}}\right]^{-1}$$
$$= \sum_{i=1}^{m-1}\sum_{j=1}^{p-1}\left[\frac{C_{ij}}{n-1}\right], \quad C_{ij} = \frac{A'_{kij}}{L'_{ijk}} \tag{7}$$

Eq. (7) only requires obtaining the value of the constant, C_{ij}, between each four-flow path lines that surround each A_{kij}, i.e. C_{ij} is constant between L_i, $L_{(i+1)j}$, $L_{i(j+1)}$, and

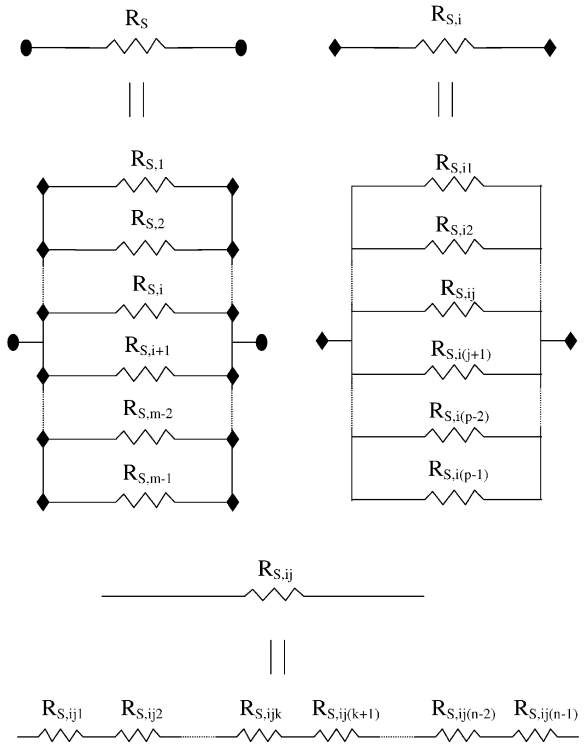

Fig. 4. An electrical network that represents the resistance to the flow in the flux network, where $S = R_s^{-1}$.

$L_{(i+1)(j+1)}$. So, this assumption simplifies Eq. (6). For further simplification second assumption must be applied.

Second assumption: *select the flow path lines, L_{ij}, so that the flow between each four-flow path lines is constant.* This assumption states that Q_{ij}, which is the flow between L_i, $L_{(i+1)j}$, $L_{i(j+1)}$, and $L_{(i+1)(j+1)}$, has a constant value for all flow pathways (ij's). So, with the help of this assumption besides Darcy's law, Eq. (7) simplifies to

$$S = R_s^{-1} = \sum_{i=1}^{m-1}\sum_{j=1}^{p-1}\frac{C_{ij}}{n-1} = \frac{(m-1)(p-1)}{n-1}C,$$
$$C = C_{ij} \quad \forall i, j \tag{8}$$

So, by applying the previous two assumptions, the relation for shape factor (Eq. (6)) is reduced to the relation illustrated in Eq. (8), where C is a constant. This relation is similar to what has been used in the graphical method for shape factor estimation in two dimensions [13,14], but the main difference between them is in the nature of the constant C.

3.2. Equivalent shape factor and the relation with the shape factor

Let us assign $\bar{S}$ as the ratio of A_{eq}, which satisfies that ΔP_k is a constant, to L_{eq}, which satisfies that Q_{ij} is a constant, i.e. applying the previous two assumptions. By assuming that the relation between A'_{kij} and L'_{ijk}, Eq. (6) is held between A_{kij} and L_{ijk}, then $\bar{S}$ can be obtained as follows:

$$\bar{S} = \frac{mp}{n}\frac{\sum_{k=1}^{n}A_k}{\sum_{i=1}^{m}\sum_{j=1}^{p}L_{ij}} = \frac{mp}{n}\frac{\sum_{k=1}^{n}\sum_{i=1}^{m-1}\sum_{j=1}^{p-1}A_{kij}}{\sum_{i=1}^{m}\sum_{j=1}^{p}\sum_{k=1}^{n-1}L_{ijk}}$$
$$= \frac{mp}{n}\frac{\sum_{k=1}^{n}\sum_{i=1}^{m-1}\sum_{j=1}^{p-1}L_{ijk}}{\sum_{i=1}^{m}\sum_{j=1}^{p}\sum_{k=1}^{n-1}L_{ijk}}C \tag{9}$$

Now dividing Eq. (8) by Eq. (9) yields

$$\frac{S}{\bar{S}} = \frac{n}{n-1}\frac{m-1}{m}\frac{p-1}{p}\frac{\sum_{i=1}^{m}\sum_{j=1}^{p}\sum_{k=1}^{n-1}L_{ijk}}{\sum_{k=1}^{n}\sum_{i=1}^{m-1}\sum_{j=1}^{p-1}L_{ijk}} \tag{10}$$

If a very condensed network has been selected, i.e. $m \gg 1$, $p \gg 1$, $n \gg 1$ and $L_{ij} \approx 0$, then Eq. (10) would state that the value of $\bar{S}$ would reach the shape factor (S) value.

4. Perfusive particle with sealing surface: derivation of the numerical procedure for the shape factor evaluation

4.1. Particle description

The perfusive particle in Pfeiffer et al. [1] can be described as perfusive particle with sealing surface as illustrated in Fig. 5A, which is a spherical particle with a portion removed to form a flat surface which will be in contact with the walls of the permeability measuring device used in Pfeiffer et al. [1]. The flat surface may result from cutting the excess amount of porous material by maintaining the particle physical and geometrical properties. The flat surface is called sealing surface because there is no flow through it. Fig. 5C represents the particle in a yz cross-sectional diagram.

According to the experimental conditions of Pfeiffer et al. [1], one hemispherical phase of the perfusive particle was subjected to a constant pressure resulting from a column of water, while the other hemispherical phase is exposed to the atmosphere, i.e. constant pressure applied to this phase. Therefore, the essential conditions, i.e. constant potential on each surface but with different potential value at each one, for applying the concept of shape factor were satisfied.

By applying the concepts of graphical method as illustrated in Holman [13] or Incropera and Dewitt [14] the perfusive particle can be divided into eight portions similar in shape and boundary conditions (Fig. 5B). The yz cross-sectional representation for the perfusive particle portion is illustrated in Fig. 5D, where the relations in the parentheses represent the dimension of the particle after normalizing with the radius a.

The shape factor of the portion of the particle in Fig. 5B will be obtained because the graphical–statistical method can be applied easily on it than using the whole perfusive particle. After that it will be related to the shape factor of

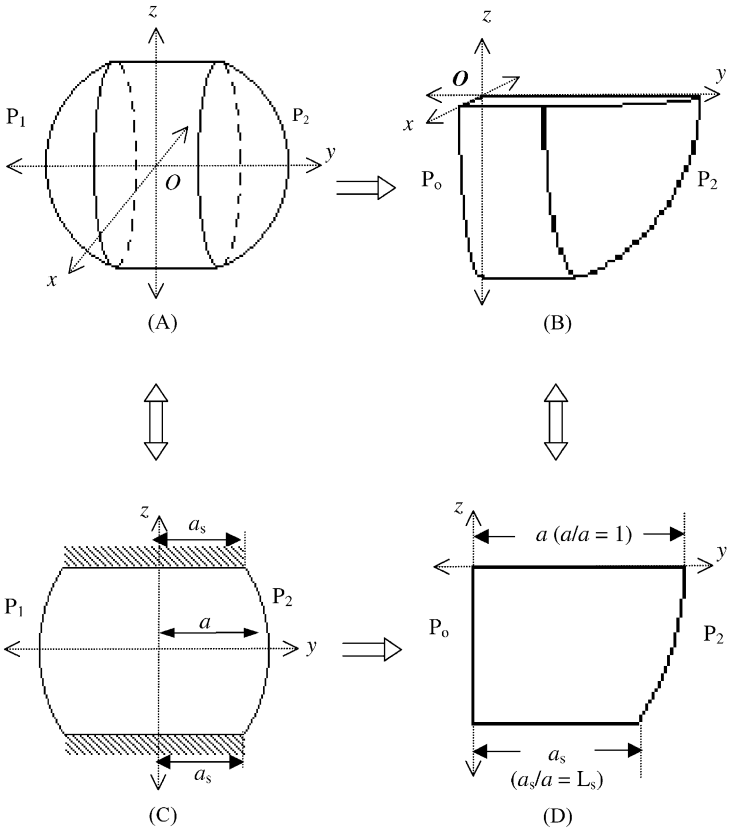

Fig. 5. (A) Perfusive particle with sealing surface under pressure drop of $\Delta P = P_2 - P_1$. (B) Perfusive particle portion that will be considered in shape factor evaluation. (C) Cross-sectional diagram for the perfusive particle with sealing surface (*yz*-plane). (D) Cross-sectional diagram for the perfusive particle potion that will be considered in shape factor evaluation (*yz*-plane).

the whole particle by a factor of 2, as will be illustrated later.

4.2. Flux network description

Before describing the flux network, the term L_{ij}, which has been used in this paper to describe the flow path line *ij*, will be used also to describe L_{ij} length whenever appropriate, i.e. L_{11} is the first flow path line, also, $L_{11} = a/a = 1$.

The distribution of L_{ij} in the *xz*-plane will be discussed first. For this plane the polar coordinate will be selected instead of the rectangular one to simplify the network as follows. If the centerline (*y*-axis) is selected as L_{11} then increasing the *i*-index in the radial direction and the *j*-index in the angular direction, then the physical projection of the network at this plane will be as in Fig. 6A. Moreover, if the nodal point in the *r*-direction is selected equal to the nodal points in the angular direction ($p = m$), then as a property of the sphere, the following relation is correct:

$$L_{i1} = L_{ij} \quad \forall j \Rightarrow \sum_{j=1}^{p} L_{ij} = \begin{cases} L_{11}, & i = 1 \\ pL_{i1} = mL_{i1}, & i > 1 \end{cases}, \quad p = m \tag{11}$$

This will reduce Eq. (9) for the equivalent shape factor to the following:

$$\bar{S} = \frac{mp}{n} \frac{\sum_{k=1}^{n} A_k}{\sum_{i=1}^{m}\sum_{j=1}^{p} L_{ij}} = \frac{m^2}{n} \frac{\sum_{k=1}^{n} A_k}{L_{11} + \sum_{i=1}^{m} mL_{i1}} = \frac{m}{n} \frac{\sum_{k=1}^{n}\sum_{i=1}^{m-1}\sum_{j=1}^{p-1} A_{kij}}{(L_{11}/m) + \sum_{i=1}^{m} L_{i1}} \tag{12}$$

Since polar coordinate has been used then the area between the index *i* and the index $i+1$, A_{ki} (Fig. 6B), can be evaluated, so the following simplification to Eq. (12) can be performed:

$$\bar{S} = \frac{m}{n} \frac{\sum_{k=1}^{n}\sum_{i=1}^{m-1} A_{ki}}{(L_{11}/m) + \sum_{i=1}^{m} L_{i1}}, \quad A_{ki} = \sum_{j=1}^{p-1} A_{kij} \tag{13}$$

As concluded in Eq. (13), the *j*-index has been omitted and we remain with the *i*-index and the *k*-index. For simplification the *j*-index will be dropped from the notation from this point in this example. Therefore, L_{ij} will be L_i and L_{ijk} will be L_{ik} and similarly for the area.

For the *yz*-plane, the flux network for perfusive particle with complete sphere shape, $L_s = 0$, can be easily predicted as illustrated in Fig. 6C. Each cross-sectional area, A_k, is considered portion of imaginary sphere surface which meet

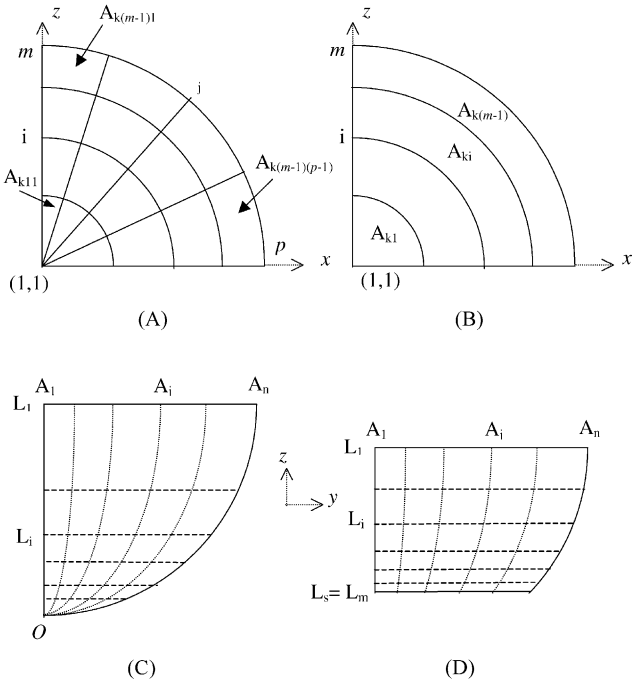

Fig. 6. (A) Flux network projection on, the perpendicular plane to the flow (*xz*-plane) with meshing in polar coordinate for the *i*-index and *j*-index. (B) The perpendicular plane to the flow (*xz*-plane) after dropping the *j*-index. (C) The parallel plane to the flow (*yz*-plane), $L_s = 0$. (D) The parallel plane to the flow (*yz*-plane), $L_s \neq 0$.

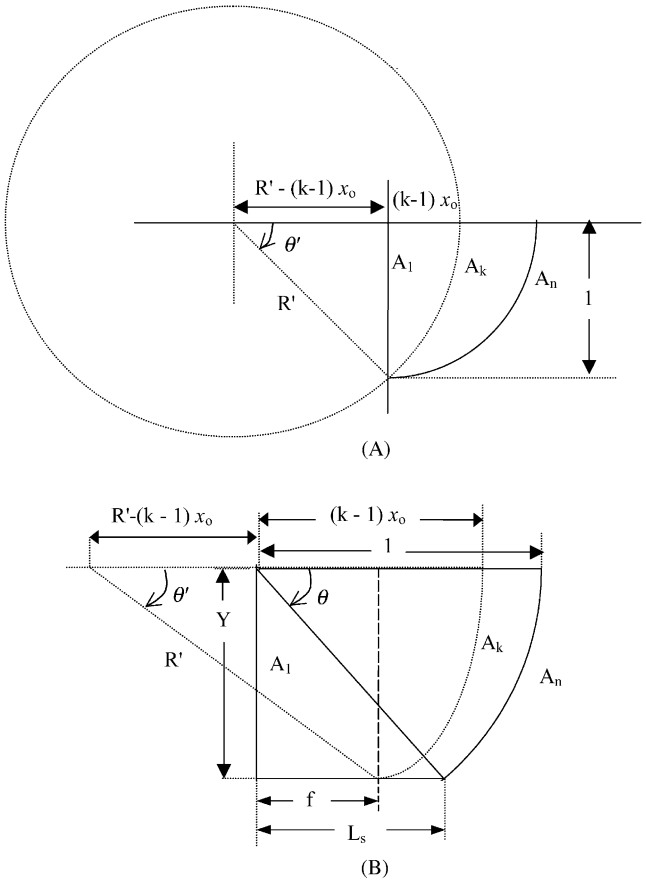

Fig. 7. Diagram used to obtain A_k relation in perfusive particle portion with sealing surface ratio, L_s: (A) $L_s = 0$; (B) $L_s \neq 0$.

with other cross-sectional areas at point O and is perpendicular to the centerline L_1. The flow path lines, L_i, are assumed to be straight lines, where distance between them is reduced as they approach the point O. Actually, the flow path lines must be curved as they approach A_n, but for practical calculations it is assumed to be straight lines as an average between the start point and the end point.

Meanwhile, *yz*-plane of the flux network for perfusive particle with sealing surface length ratio of L_s, $L_s = a_s/a$, not equal to zero is illustrated in Fig. 6D. The cross-sectional area A_k is considered as part of imaginary sphere surface. These imaginary spheres are perpendicular to the centerline L_1 and they not necessarily meet at point O, as in complete sphere, but they intersect the line L_s at a position where the pressure drop in the perfusive particle is satisfied. The flow path lines, L_i, are assumed to be straight lines as in the complete sphere ($L_s = 0$), where distance between them is reduced as they approach line L_s.

4.3. Area relation (A_k)

The expression for A_k as a function of the dimensionless sealing surface length L_s, is obtained as follows. Since we deal with porous media and a straight line is assumed to represent the flow path line, a uniform pressure drop can be assumed within the perfusive particle, $\partial P/\partial y$ is a constant. Thus, the *n* cross-sectional areas will divide each flow path line to $n - 1$ equal segments, each of them equal to L_{i1}, in order to have constant pressure drop between any two consecutive cross-sectional areas. For the special centerline L_1, the value of L_{11} would be equal to $x_0 = (n-1)^{-1}$.

For complete sphere, i.e. no sealing surface ($L_s = 0$), Fig. 7A illustrates the relation between the area A_k and the perfusive particle portion under consideration. In Fig. 7A, R' is the radius of the sphere of which A_k is a portion of its surface. R' is not fixed but is a function of *k*, i.e. if $k = n$ then $R' = L_1$, and if $k = 1$ then $R' = \infty$. The expression for A_k for complete sphere ($L_s = 0$) can be obtained by using simple geometric relations, which will conclude the following relation for A_k:

$$A_k = \frac{\pi}{4}\left[1 + \frac{(k-1)^2}{(n-1)^2}\right] = \frac{\pi}{4}[(1-W) + 2W],$$
$$W = \frac{(k-1)^2}{(n-1)^2} \tag{14}$$

The cross-sectional area A_1 ($k = 1$) is an area of a quarter of a circle with radius of magnitude equal to 1; therefore, A_1 is equal to $\pi/4$. On the other hand, the cross-sectional area A_n ($k = n$) is the area of one-eighth of a sphere with radius of magnitude equal to 1; therefore, A_n is equal to $\pi/2$. The previous two cross-sectional areas are the two extremes

for the value of A_k. So, the right-hand side of Eq. (14) proposes, a weight function, W, which is used as follows: A_1 is multiplied by $1 - W$ and A_n is multiplied by W, then they are summed up. This summation gives the left-hand side of Eq. (14), where W is equal to $(k-1)^2/(n-1)^2$, i.e. W is equal to 0 at $k = 1$ and W is equal to 1 at $k = n$.

For $L_s \neq 0$, A_1, A_k, and A_n can be obtained from Fig. 7B using geometrical relations, where Y is the distance between L_1 and L_s. Expression for A_k will be

$$A_k = \int_0^{\pi/2}\int_0^{\theta'} (R')^2 \sin\theta \, d\theta \, d\phi = \frac{\pi}{4}[Y^2 + [(k-1)x_0 - f]^2] \quad (15)$$

As observed from Eq. (15), a relation between f and L_s is required to obtain A_k expression as a function of L_s, k, and n. As mentioned in the description of A_k in the flux network description, the intersection point between A_k and L_s should satisfy the pressure drop in the particle. Since, a constant pressure drop is assumed in the particle, $\partial P/\partial y$ is a constant, and since A_k is selected in a way to have constant pressure drop between each consecutive cross-sectional area, then L_s will be divided into $n-1$ equal segments. Therefore, the position of the intersection point between A_k and L_s will be $(k-1)L_s/(n-1)$ far from the intersection point of L_s and A_1, i.e. $f = (k-1)L_s/(n-1)$. So, by substituting $x_0 = (n-1)^{-1}$, $Y^2 = 1 - L_s^2$, and $f = (k-1)L_s/(n-1)$ in Eq. (15) and rearranging, Eq. (16) will be obtained (detailed derivation as shown in Appendix A).

$$A_k = \frac{\pi}{4}[(1-W)(1-L_s^2) + 2W(1-L_s)], \quad W = \frac{(k-1)^2}{(n-1)^2} \quad (16)$$

As observed, Eq. (16) has the similar general formula used in Eq. (14), i.e. $A_k = [(1-W)A_1 + 2WA_n]$.

4.4. Flow path length (L_i)

The expression for L_i is derived using Fig. 8, where Y_i is the distance between L_1 and L_i and y_i is the distance between L_i and L_{i+1}. L_i can be obtained easily by using the triangle properties (Eq. (17)). Y is the sum of all y_k's between L_1 and L_i (Eq. (18)).

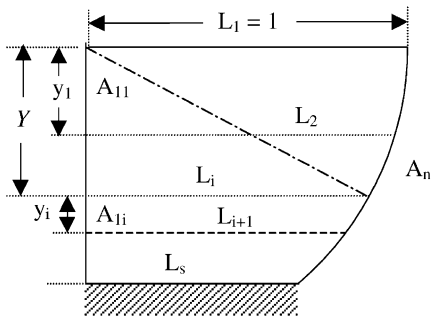

Fig. 8. Schematic diagram for the perfusive particle portion with sealing surface ratio of L_s that was used to obtain the relation for L_i.

$$L_i^2 = 1 - Y_i^2 \quad (17)$$

$$Y_i = \sum_{v=1}^{i-1} y_v \quad (18)$$

So, the problem is no longer finding L_i's but instead finding y_i's. The relation between different y_i's can be obtained using the assumption that the flow Q_i is constant between any two consecutive flow path lines, thus resulting the relation in Eq. (19). Since the pressure drop in the perfusive particle is assumed to be constant and hence the distance between the A_k's is taken to be constant, i.e. $L_i = (n-1)L_{i1}$, and since $x_0 = (n-1)^{-1}$ then $L_{i1} = L_i x_0$. Also, since A_{11} is the area of a quarter of a circle (Fig. 6B) with radius of y_1, then the expression for A_{1i} would be as in Eq. (20).

$$A_{1i} = \frac{L_{i1}}{L_{11}} A_{11} = \frac{L_{i1}}{x_0} A_{11} \quad (19)$$

$$A_{1i} = \tfrac{1}{4}\pi y_1^2 (1 - Y_i^2)^{0.5} \quad (20)$$

On the other hand, A_{1i} is the area that represents the difference between two other quarter circle areas as illustrated in Fig. 6B and represented by Eq. (21). By equating Eqs. (20) and (21), an expression for y_i will be obtained (Eq. (22)). Therefore, L_i can be obtained through Eqs. (17), (18) and (22), but the only required information to initiate the calculation procedure is y_1, which should be as small as possible to validate all the assumptions.

$$A_{1i} = \tfrac{1}{4}\pi[(Y_i + y_i)^2 - Y_i^2] \quad (21)$$

$$y_i = -Y_i + \sqrt{Y_i^2 + y_1^2(1 - Y_i^2)^{0.5}} \quad (22)$$

4.5. Summary

Since all the previous relations for A_k and L_i are based on dimensionless length, then the equivalent shape factor value for the perfusive particle portion, $\bar{S}_{\text{portion}}$, is obtained as in Eq. (23). Note that, the value of the equivalent shape factor, $\bar{S}_{\text{portion}}$, will approach the value of the shape factor of the perfusive particle portion, S_{portion}, as m and n increased, i.e. x_0 and y_1 decreased.

$$\frac{\bar{S}_{\text{portion}}}{a} = \frac{m}{n}\frac{\sum_{j=1}^{n} A_j}{\sum_{i=1}^{m} L_i},$$
$$A_k = \frac{\pi}{4}[(1-W)(1-L_s^2) + 2W(1-L_s)],$$
$$W = \frac{(k-1)^2}{(n-1)^2},\ n-1 = \frac{1}{x_0},$$
$$L_i^2 = 1 - Y^2,$$
$$Y = \sum_{v=1}^{i-1} y_v,\ y_v = -Y + \sqrt{Y^2 + y_1^2(1-Y^2)^{0.5}} \quad (23)$$

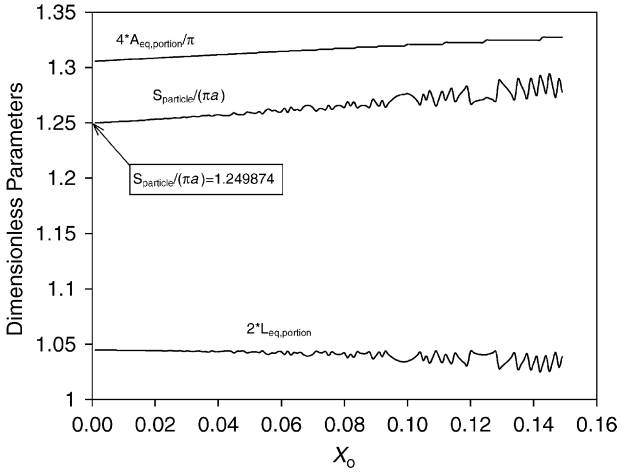

Fig. 9. Results of simulation for perfusive particle with $L_s = 0.04$. $A_{eq,portion}$ and $L_{eq,portion}$ are the equivalent average area and the equivalent average length of the perfusive particle portion, respectively.

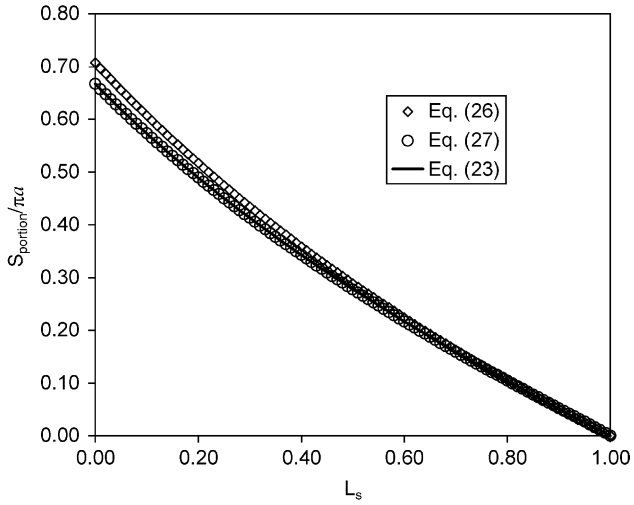

Fig. 10. Shape factor of perfusive particle with sealing surface length ratio of L_s computed by different methods developed in the paper.

In order to obtain the value of the equivalent shape factor of the whole particle, the equivalent shape factor in Eq. (23) must be multiplied by 2. Because, in the whole particle, the flow will pass a cross-sectional area four times greater than the cross-sectional area of the derived portion, and will flow twice the length of the portion, as shown in Fig. 5. Therefore, $S_{particle} = 2S_{portion}$.

For example, the equivalent shape factor value of a perfusive particle, $\bar{S}_{particle}$, with $L_s = 0.04$ has been simulated from $x_0 = 0.15$ to $x_0 = 0.001$ using $y_1 = x_0$. The results are shown in Fig. 9, where the division of $4A_{eq,portion}/\pi$ over $2L_{eq,portion}$ yields $2\bar{S}_{portion}/(\pi a)$, which is $\bar{S}_{particle}/(\pi a)$. The results (Fig. 9) show that as x_0 decreases, the equivalent shape factor value, $\bar{S}_{particle}$, changes until it becomes independent of x_0 value, where its value becomes the value of the shape factor, S. This observation will validate our assumptions related to the convergence of the equivalent shape factor.

The previous derived technique (Eq. (23)) requires the simulation of the equivalent shape factor, until its value becomes independent of x_0 and y_1, i.e. $\bar{S}_{particle} = S_{particle}$. This step may require a long simulation time. Therefore, calculating $S_{particle}$ value as function of L_s and a in terms of single or multiequations will be very helpful in many applications. Therefore, the value of $S_{particle}$ obtained through Eq. (23), will be used as the experimental values for the next section of the paper.

5. Perfusive particle with sealing surface: derivation of the mathematical expression for the shape factor

Providing a mathematical expression to calculate the shape factor is more practical and beneficial for permeability calculation than the one from simulation or graphs. Therefore, developing a simple mathematical expression for shape factor of perfusive particle with sealing surface of length ratio of L_s is the objective of this section of the paper.

In developing the mathematical expression, the geometrical method [16], was used. The shape factor of the perfusive particle portion illustrated in Fig. 5B was estimated as follows.

Considering the shape factor, if the average area is selected to be the square root of the product of the area at the center of the particle, A_1, by surface area, A_n (Eq. (24)). Then to obtain the average flow path length, different types of averaging methods were tried, and it was found that the arithmetic average between L_s and $L_1 = 1$ (Eq. (25)) gives the best shape factor values, as compared with the simulated ones (Eq. (23)) as shown in Fig. 10.

$$A_{avg} = \sqrt{A_1 A_n} = \sqrt{\left[\tfrac{1}{4}\pi(1 - L_s^2)\right]\left[\tfrac{1}{2}\pi(1 - L_s)\right]} \quad (24)$$

$$L_{avg} = \tfrac{1}{2}(1 + L_s) \quad (25)$$

$$S_{portion} = \frac{\pi a}{\sqrt{2}} \frac{[(1 - L_s^2)(1 - L_s)]^{0.5}}{1 + L_s} \quad (26)$$

As observed from Fig. 10, the proposed expression for the shape factor converges to the simulated values as the value of L_s reaches 1. This behavior of the shape factor expression suggests a couple of adjustments to the power and the coefficient values in Eq. (26).

By using the nonlinear regression package in STATGRAPHIC® program, the proposed expression fits the simulated shape factor values, Eq. (23) with high values of m and n, perfectly if Eq. (27) is used. For the whole particle, the shape factor expression would be Eq. (28).

$$S_{portion} = \frac{\pi a}{1.5} \frac{[(1 - L_s^2)(1 - L_s)]^{0.48153}}{1 + L_s} \quad (27)$$

$$S_{particle} = 2S_{portion} = \frac{4\pi a}{3} \frac{[(1-L_s^2)(1-L_s)]^{0.48153}}{1+L_s} \quad (28)$$

Eq. (28) is valid for any perfusive particle with radius equal to a and sealing surface length ratio of L_s, resulting from removing the excess material from the original perfusive particle, where it experiences a constant pressure drop inside the particle and is subjected to constant pressure value at each boundary, but they differ in their values, as illustrated in Fig. 5A.

6. Comparison of experimental permeability of perfusive particle with the results from shape factor

Air at 26 °C with an absolute viscosity, μ, of 1.86×10^{-5} Pa s was used in Pfeiffer et al. [1] to measure the volumetric flow rate through a perfusive particle with diameter equal to 50 μm at different pressure drops, as shown in Fig. 1. According to their CFD simulation results, the interstitial permeability of the perfusive particle, $K_{Pi} = K_P/\varepsilon_P$, was equal to 7.63×10^{-15} m^2. Since the reported porosity of the perfusive particle, ε_P, was equal to 0.5, the permeability of the perfusive particle used will be equal to 3.815×10^{-15} m^2.

According to their experimental conditions, Darcy's law is the appropriate relation to describe the flow inside the perfusive particle. According to Darcy's law, Eq. (3) can be used to obtain the permeability, where the ratio $Q/(-\Delta P)$ is the slope that would be obtained experimentally. In the considered example, the obtained slope from Fig. 1 is equal to 1.98×10^{-14} m^3/Pa. A perfusive particle with 50 μm in diameter and sealing surface of length ratio 0.04 ($L_s = 0.04$) was used in those experiments. In the CFD simulation, the particle was represented by easily removing the excess material to form L_s. So Eq. (28) can be used to estimate the shape factor, which yield a shape factor value, S, of $31.428\pi \times 10^{-6}$ m. Applying Eq. (3), a value of 3.73×10^{-15} m^2 for the permeability of the perfusive particle is obtained, which yields an interstitial permeability of 7.46×10^{-15} m^2 for a perfusive particle with porosity of 0.5. These results are in a good agreement with Pfeiffer et al. [1], which is based on CFD simulation.

Therefore, using the shape factor technique allows permeability calculation without the use of the complicated CFD simulation. Moreover, the shape factor technique is not limited to a certain range of particle diameter, porosity, and/or sealing surface length ratio (L_s), i.e. Fig. 2, while those parameters were limiting factors in Pfeiffer et al. [1].

7. Summary and conclusion

A modified graphical–statistical method to estimate the shape factor of three-dimensional bodies has been presented and proved by using electrical network approach. This method can be used to calculate the shape factor of any body subjected to constant potential difference between its faces regardless of the potential type, i.e. it can be used with voltage difference, pressure difference, temperature difference, concentration difference, etc. This method requires a suitable way to calculate the area perpendicular to the flow and the flow path line length separately.

As an example, the permeability of a perfusive particle has been measured successfully by using the presented shape factor technique. The shape factor for a perfusive particle with sealing surface length ratio of L_s has been obtained and correlated (Eq. (28)) using the modified graphical–statistical method. This technique has proved to be simple and practical, in comparison with other published techniques. Only a few experiments are required to obtain the flow through a perfusive particle as the pressure drop across the perfusive particle changes, i.e. Q versus $-\Delta P$. From the obtained data and the physical conditions of the perfusive particle through these experiments, Eqs. (3) and (28) can be used to obtain the permeability of the perfusive particle. This approach shows excellent agreement with the numerical CFD simulation approach of Pfeiffer et al. [1]. Moreover, the proposed shape factor approach (Eqs. (3) and (28)) for evaluating perfusive particle permeability is not limited to a certain values of the particle radius, porosity, and/or values of the sealing surface length ratio, L_s.

Appendix A

The area, A_k, in relation to the sealing surface length ration, L_s (Eq. (16)) is obtained by using Fig. 7B as follows. Area, A_k, can be calculated using Eq. (A.1). Expressions for R' and $\cos\theta'$ as functions of L_s, k, and n are required.

$$A_k = \int_0^{\pi/2}\int_0^{\theta'} (R')^2 \sin\theta' \, d\theta \, d\phi = \frac{\pi}{2}(R')^2(1-\cos\theta') \tag{A.1}$$

By applying the Pythagorean theorem, the following expression that relates R' to f, k, Y, and x_0 will be obtained as illustrated below:

$$\begin{aligned}(R')^2 &= [R' - (k-1)x_0 + f]^2 + Y^2 \\ &= (R')^2 - 2R'[(j-1)x_0 - f] \\ &\quad + [(j-1)x_0 - f]^2 + Y^2\end{aligned} \tag{A.2}$$

therefore,

$$R' = \frac{[(k-1)x_0 - f]^2 + Y^2}{2[(k-1)x_0 - f]} \tag{A.3}$$

For $\cos\theta'$, the trigonometric relation implies that

$$\cos\theta' = \frac{R' - (k-1)x_0 + f}{R'} = 1 - \frac{(k-1)x_0 - f}{R'} \tag{A.4}$$

Now substituting (A.4) in Eq. (A.1) yields

$$\begin{aligned} A_k &= \frac{\pi}{2}(R')^2(1-\cos\theta') \\ &= \frac{\pi}{2}(R')^2\left[1-\left(1-\frac{(k-1)x_0-f}{R'}\right)\right] \\ &= \frac{\pi}{2}(R')^2\left(\frac{(k-1)x_0-f}{R'}\right) \\ &= \frac{\pi}{2}R'[(k-1)x_0-f] \end{aligned} \tag{A.5}$$

Now substituting for R' from Eq. (A.3) in Eq. (A.5) yields

$$\begin{aligned} A_k &= \frac{\pi}{2}\left[\frac{[(k-1)x_0-f]^2+Y^2}{2[(k-1)x_0-f]}\right][(k-1)x_0-f] \\ &= \frac{\pi}{4}[[(k-1)x_0-f]^2+Y^2] \end{aligned} \tag{A.6}$$

Now substituting $x_0=(n-1)^{-1}$, $f=(k-1)L_s/(n-1)$, and $Y^2=1-L_s^2$ yields

$$\begin{aligned} A_k &= \frac{\pi}{4}[[(k-1)x_0-f]^2+Y^2] \\ &= \frac{\pi}{4}\left[\left[\frac{k-1}{n-1}-\frac{(k-1)L_s}{n-1}\right]^2+1-L_s^2\right] \\ &= \frac{\pi}{4}\left[\frac{(k-1)^2}{(n-1)^2}[1-L_s]^2+1-L_s^2\right] \\ &= \frac{\pi}{4}\left[W[1-L_s]^2+1-L_s^2\right], \\ W &= \frac{(k-1)^2}{(n-1)^2} \end{aligned} \tag{A.7}$$

Rearranging Eq. (A.7) as follows will yield Eq. (16).

$$\begin{aligned} A_k &= \tfrac{1}{4}\pi[W[1-L_s]^2+1-L_s^2] \\ &= \tfrac{1}{4}\pi[W(1-2L_s+L_s^2)+1-L_s^2] \\ &= \tfrac{1}{4}\pi[W-2WL_s+WL_s^2+1-L_s^2] \\ &= \tfrac{1}{4}\pi[W-2WL_s+WL_s^2+1-L_s^2+(W-W)] \\ &= \tfrac{1}{4}\pi[(2W-2WL_s)+(WL_s^2-W)+(1-L_s^2)] \\ &= \tfrac{1}{4}\pi[2W(1-L_s)-W(1-L_s^2)+(1-L_s^2)] \\ &= \tfrac{1}{4}\pi[2W(1-L_s)+(1-W)(1-L_s^2)] \end{aligned} \tag{A.8}$$

References

[1] J.F. Pfeiffer, J.C. Chen, J.T. Hsu, Permeability of gigaporous particles, AIChE J. 42 (1996) 932–939.

[2] N.B. Afeyan, N.F. Gordon, I. Mazsaroff, L. Varady, S.P. Fulton, Y.B. Yang, F.E. Regnier, Flow-through particles for the high perfo-rmance liquid chromatographic separation of biomolecules: perfusion chromatography, J. Chromatogr. 519 (1990) 1–29.

[3] A.I. Liapis, Y. Xu, O.K. Crosser, A. Tongta, Perfusion chromatography. The effects of intraparticle convective velocity and microsphere size on column performance, J. Chromatogr. A 702 (1995) 45–57.

[4] A.I. Liapis, M.A. McCoy, Theory of perfusion chromatography, J. Chromatogr. 599 (1992) 87–104.

[5] A.E. Rodrigues, J.M. Loureiro, C. Chenou, M. Rendueles de la Vega, Bioseparation with permeable particles, J. Chromatogr. B 664 (1995) 233–240.

[6] M. McCoy, K. Kalghatgi, F.E. Regnier, N. Afeyan, Perfusion chromatography—characterization of column packings for chromatography of proteins, J. Chromatogr. 743 (1996) 221–229.

[7] M. Rendueles de la Vega, C. Chenou, J.M. Loureiro, A.E. Rodrigues, Mass transfer mechanisms in Hyper D. media for chromatographic protein separation, Biochem. Eng. J. 1 (1998) 11–23.

[8] A.E. Rodrigues, J.C. Lopez, Z.P. Lu, J.M. Loureiro, M.M. Dias, Importance of intraparticle convection in the performance of chromatographic processes, J. Chromatogr. 590 (1992) 93–100.

[9] G. Neale, N. Epsteine, W. Nader, Creeping flow relative to permeable spheres, Chem. Eng. Sci. 28 (1973) 1865–1874.

[10] R.H. Davis, H.A. Stone, Flow through beds of porous particles, Chem. Eng. Sci. 48 (1993) 3993–4005.

[11] H.S. Carslaw, J.C. Jaeger, Conduction of Heat in Solids, 2nd Edition, Clarendon Press, Oxford, 1959.

[12] M. Chung, P.S. Jung, R.H. Rangel, Semi-analytical solution for heat transfer from a buried pipe with convection on the exposed surface, Int. J. Heat Mass Transfer 42 (1999) 3771–3786.

[13] J.P. Holman, Heat Transfer, 7th Edition, McGraw-Hill, New York, 1990, pp. 79–86.

[14] F.P. Incropera, D.P. Dewitt, Introduction to Heat and Mass Transfer, 3rd Edition, Wiley, New York, 1996, pp. 169–173.

[15] J.C. Smith Jr., J. Lind, D. Lermond, Shape factors for conductive heat flow, AIChE J. 4 (1958) 330–331.

[16] M. Nickolay, L. Fischer, H. Martin, Shape factors for conductive heat flow in circular and quadratic cross-sections, Int. J. Heat Mass Transfer 41 (1998) 1437–1444.

[17] I. Langmuir, E.Q. Adams, G.S. Meikle, Flow of heat through furnace walls: the shape factor, Trans. Am. Electrochem. Soc. 24 (1913) 53–81.

[18] I. Anteby, I. Shai, Modified conduction shape factors for isothermal bodied embedded in a semi-infinite medium, Numer. Heat Transfer 23 (1993) 233–245.

[19] E. Hahne, U. Grigull, Shape factor and shape resistance for steady multi-dimensional heat conduction, Int. J. Heat Mass Transfer 18 (1975) 751–767.

[20] G.K. Lewis, Shape factors in conduction heat flow for circular bars and slabs with various internal geometries, Int. J. Heat Mass Transfer 11 (1967) 985–992.

[21] J.E. Sunderland, K.R. Johnson, Shape factors for heat conduction through bodies with isothermal or convective boundary conditions, ASHRE Trans. 70 (1964) 237–241.

[22] R.B. Chapuis, Shape factors for permeability tests in boreholes and bizometers, Groundwater 27 (1989) 647–654.

[23] F. Tavenas, M. Diene, S. Leroueil, Analysis of the in situ constant head permeability test in clays, Can. Geotech. J. 27 (1990) 305–314.

[24] E.G. Youngs, G. Spoor, G.R. Goodall, Infiltration from surface ponds into soils overlaying a very permeable substratum, J. Hydrol. 186 (1996) 327–334.

[25] M.M. Yovanovich, Dimensionless shape factors and diffusion lengths of three-dimensional bodies, in: Proceedings of the ASME/JSME Thermal Engineering Conference, Lahaina, Maui, Hawaii, March 19–24, 1995, pp. 103–114.